P2.27 AEROSOL OPTICAL DEPTH ANALYSIS WITH NOAA GOES AND POES IN THE WESTERN ATLANTIC

Arunas P. Kuciauskas* and Douglas L. Westphal
Naval Research Laboratory
Monterey, California

Philip A. Durkee
Naval Postgraduate School
Monterey, California

1. INTRODUCTION

Monitoring tropospheric aerosols on a global scale is essential for evaluating the earth's radiation budget. There is a developing interest to globally quantify aerosol properties on fine spatial and temporal scales. Thus far, this analysis has proven to be a daunting task, since most established aerosol sensing techniques are land-based, providing poor spatial and temporal coverage. Higurashi *et al*. (1999) suggests that aerosol concentration, size distribution, composition, and optical properties will have to be measured globally, and that satellite remote sensing is an effective tool for such a task. Over the past few decades, scientists have developed algorithms to convert satellite upwelling radiances into aerosol properties such as optical depth.

This study focuses on one such algorithm developed by Durkee *et al*. (1991) (hereafter referred to as the Naval Postgraduate School (NPS) algorithm). The NPS algorithm is applied to AVHRR data within a cloud-free, single scatter environment. By using the ratio of channel 1 and 2 radiances, an estimate of the aerosol size distribution is extracted. During three recent field campaigns, Durkee *et al*. (1999) show that the NPS algorithm performs well for aerosol optical depth (AOD) below about 0.4 at 0.63μm wavelength. The results only provided snapshots of the experimental regions, however, since AVHRR passes over a particular region a few times per day. Recently, both the AVHRR and the Geosynchronous Operational Environmental Satellite (GOES) satellites were applied to the NPS algorithm in order to provide temporal coverage of AOD over specified experimental regions. For GOES AOD processing, an aerosol model index (AMI) must be obtained from AVHRR data. Therefore, the passes between NOAA and GOES must be close in time for the NOAA-generated AMI to be valid for GOES-processed AOD. The current research addresses the following:

- Proper radiance calibration of the visible sensor of GOES
- Validation of the AOD derived from NOAA and GOES-8
- Evaluation of the phase function parameters used in the retrieval algorithm

2. DATA

2.1 *NOAA Advanced Very High Resolution Radiometer (AVHRR)*

The AVHRR instruments onboard the NOAA-14 and NOAA-16 satellites provided the data for the polar orbiter component of this study. Over the experimental region, the NOAA-16 AVHRR provided the local afternoon data while the NOAA-14 AVHRR provided data late in the afternoon. The data from the NOAA-14 was at times questionable due to low sun angle problems. Therefore, the NOAA-16 data was the more reliable dataset.

2.2 *GOES-8 Imager*

The GOES-8 imager data was used for the geostationary satellite component of this study. For this research, only the visible channel (channel 1) data was used for the AOD calculations. Compared to the AVHRR, the GOES dataset was much noisier and required several steps of adjustments before the data was comparable to the expected radiances. Section 4 describes these correction techniques.

2.3 *AERONET Sun - sky Scanning Spectral Radiometer*

Data collected from the Aerosol Robotic NETwork (AERONET) automated radiometers are applied as ground truth of AOD for this study. The AOD measurements are made in 8 spectral bands, of which the 670 nm wavelength data is comparable to that used in the optical depth calculation obtained from both the GOES and NOAA retrievals. A thorough description of AERONET can be found in Holben *et al.* 1998.

* *Corresponding author address:* Arunas P. Kuciauskas, Naval Research Laboratory, Monterey, CA 93943
e-mail: kuciauskas@nrlmry.navy.mil

AERONET data were obtained from radiometer instruments installed on three island sites: eastern Bermuda, (U.K.) (32 22'N/64 41'W), La Paguera, Puerto Rico (17 58'N/67 02'W) and Guadaloupe, Island (Fr.) (16 19'N/61 30'W), all within the western Atlantic Basin (see Fig. 1).

3. METHODOLOGY

3.1 *GOES-8 Calibration and Correction Processes*

Figure 2 displays an example of radiance comparisons between the calibrated GOES and AVHRR datasets and illustrates the problem associated with GOES noise. The image passes occurred at a similar time and were registered over the same 100 km by 100 km domain surrounding Bermuda. In addition, both satellites had similar viewing geometries (scatter angles were ± 0.1° of each other). The atmospheric conditions immediately south of Bermuda (outlined in red) were clear and homogeneous at this time. The panels on the right side in Fig. 2 are frequency distributions of radiances that were extracted within the outlined region within the left panels. As expected, the

Figure 1. Map of the experimental region with locations of the AERONET stations: Bermuda, La Paguera, and Guadaloupe.

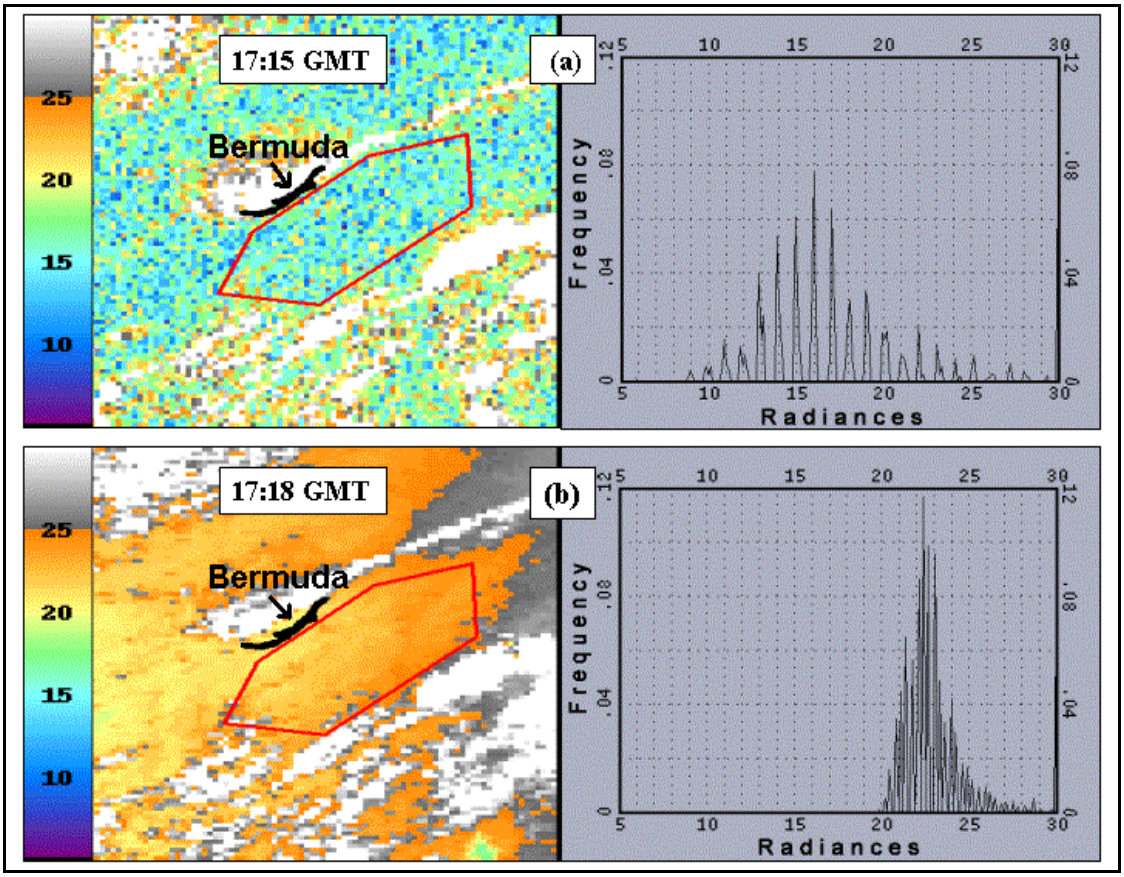

Figure 2. Comparisons of radiance images and associated frequency of radiance histograms between (a) GOES-8 and (b) NOAA-16 on 02 September 2001. Histograms were developed from areas within red annotations. Radiances, as shown within the color legend and the histogram X axis, are in units of $Wm^{-2}sr^{-1}\mu m^{-1}$.

image in Fig. 2b displays a relatively homogeneous field of radiances; its corresponding frequency histogram displays shows a pronounced signal peak with a narrow radiometric width, indicative of the pristine atmospheric conditions. In contrast, the GOES-8 sensor, situated in an orbit that is 40 times the distance of the NOAA sensor, produces an image (shown in Fig. 2a) that is significantly noisier; its corresponding histogram profile displays a weaker signal peak and wider radiometric range. As atmospheric conditions become hazier, the GOES-8 peak signal and radiometric resolutions become even less discernable, thus complicating the processed AOD calculations. In addition, the GOES-8 signal peak at ~ 16 $Wm^{-2}sr^{-1}\mu m^{-1}$ is significantly weaker than the NOAA-16 signal peak at ~22.5 $Wm^{-2}sr^{-1}\mu m^{-1}$, thus necessitating a further correction factor to GOES-8.

For this study, in order to match GOES with NOAA data during AOD processing, two correction techniques were applied to the GOES channel 1 radiance data. Dr. C. R. N. Rao (personal communication in July, 2000) provided the first correction technique; a calibration methodology of GOES-8 channel radiance by a vicarious technique. Details of this method can be found in Rao and Zhang (1999) and Rao et al. (1999).

A preliminary assessment of the calibrated GOES data indicated that its resulting AOD values were significantly higher than the NOAA-generated AOD as well as the AERONET observations of AOD. Therefore, a further correction method was applied, as discussed below.

The correction technique involved comparisons between GOES-8 and NOAA-16 channel 1 radiances, whose wavelengths, centered on 0.65 and 0.63 mm, respectively, were similar. Figure 3 presents the comparisons over 296 pairs of GOES and NOAA channel 1 radiances. As shown, the radiance ranged along the low end of the radiance spectrum (0 to 40 $Wm^{-2}sr^{-1}\mu m^{-1}$) which is where the detection of aerosols would occur. As shown, there was very poor correlation between the NOAA and GOES data, due to the large noise problem in GOES. As a plausible correction, it was decided to perform a manually-determined selection of the "center of mass" within the domain shown in Figure 3. Using the Cartesian coordinates, the selected center of mass of the distribution was positioned at point Y (NOAA axis) = 24.0 $Wm^{-2}sr^{-1}\mu m^{-1}$ and point X (GOES axis) = 19.0 $Wm^{-2}sr^{-1}\mu m^{-1}$.

Assuming there is a linear relationship between the channel 1 radiances of GOES and NOAA, the correction factor was determined by locating the X (GOES) intercept from the slope (red dashed line), which was estimated to be 5.5 $Wm^{-2}sr^{-1}\mu m^{-1}$. Therefore, before the actual AOD processing took place, the correction factor was added to the calibrated value of the GOES channel 1 radiation.

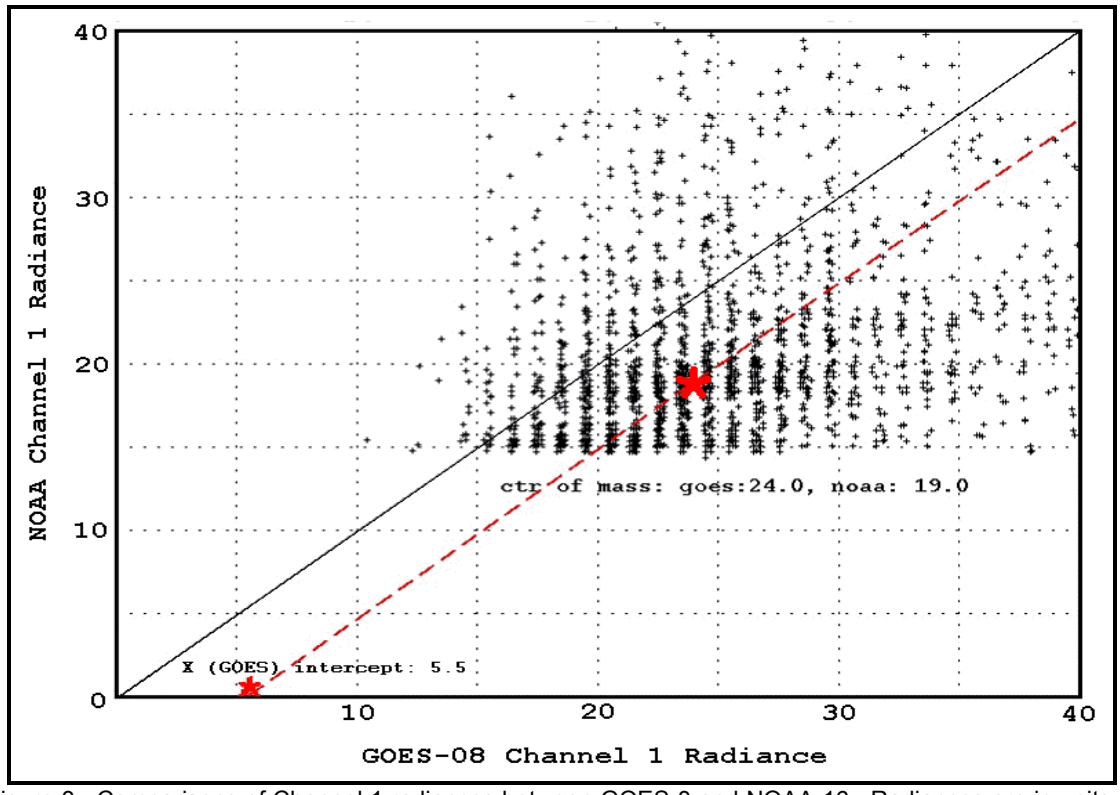

Figure 3. Comparisons of Channel 1 radiances between GOES-8 and NOAA-16. Radiances are in units of $Wm^{-2}sr^{-1}\mu m^{-1}$.

3.2 *AOD RETRIEVAL FROM SATELLITE DATA*

Figure 4 displays a flowchart to the steps involved in the processing of the satellite data. The NPS algorithm was developed by Brown (1997), and then modified by Smith (1998) and Kuciauskas (2002). It consists of 3 major parts: pre-processing, processing, and post-processing. For the pre and post-process stages, a combination of Terascan, Cshell and PERL software manipulate the data. During the processing stage, the satellite data is processed and converted to AOD values by code written in FORTRAN 77.

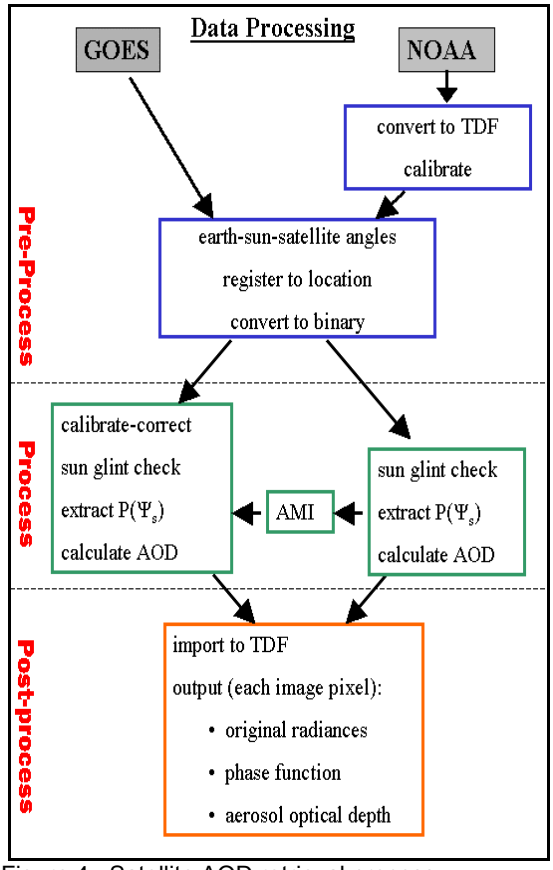

Figure 4. Satellite AOD retrieval process.

AOD is calculated using a simplified form of the radiative transfer equation:

$$\delta_a = \left(4\mu L_a\right) \Big/ \left(\omega_o F_o p(\psi_s)\right).$$

The cosine of the satellite zenith angle (μ), the single-scatter albedo (ω_o), and the solar radiance (F_o) are all constants. Radiance due to aerosol scatter (L_a), is mathematically straightforward and is described in detail by Brown (1997). The scattering phase function, $p(\psi_s)$, is obtained from a process described below.

Obtaining the scattering phase function values requires knowledge of the aerosol characteristics and size distribution, which is not routinely available. Therefore, the scattering phase function must be parameterized. Durkee *et al.* (1991) develop the parameterization technique consisting of calculating the ratio of the NOAA channel 1 and 2 radiances, 'S_{12}'. The scattering efficiency (Q_{scat}) of an aerosol distribution is wavelength dependent and peaks when the radius of the aerosol particle is nearly equal to that of the radiation wavelength. As a result, S_{12} will be larger for smaller size particle distributions and smaller for larger size aerosol particle distributions. S_{12} varies from pixel to pixel. Therefore, variations in the aerosol size distribution can be detected within the pixel resolutions of the satellite image data.

4. RESULTS

For this study, 22 cases were selected to analyze the performance of the NPS algorithm in providing satellite-derived AOD calculations. Section 5.1 discusses one case study within a dust environment.

4.1 *CASE 18 SEPTEMBER 2001. HIGH AOD CONDITIONS OVER GUADALOUPE ISLAND*

During the summer months, dust generated from the African deserts is often propagated across the southern latitudes of the Atlantic Ocean basin by the easterly trade winds, oftentimes impacting the visibility and aerosol characteristics over regions of the Caribbean and the east coast of the US.

The GOES-8 image in Figure 5 displays a large region of Saharan dust surrounding the Guadaloupe Island region (inside the annotated box). A large cloud mass just to the north of Guadaloupe Island region eventually propagated south over the study region, which impacted some of the AOD measurements later in the day.

Figure 6 presents the AOD images generated by the NPS algorithm on both NOAA-16 and GOES-8 data. The time range for this study is from 1645 UTC through 2045 UTC. The data from NOAA-16 at 17:50 UTC and NOAA-14 at 21:16 UTC provided the AMI to the GOES AOD calculations. The locations of AOD measurements are shown by the annotated red boxes. A large cloud field is shown to be propagating southward toward Guadaloupe Island throughout the time period. As a result, AOD measurements between 19:15 and 20:15 UTC were omitted due to cloud contamination. As shown, AOD values range from 0.33 to 0.48. As the cloud field began impacting the Guadaloupe Island region, measurements of AOD became increasingly difficult after 18:45 UTC.

Figure 7 presents the time series of AOD for this case. Both the GOES-generated AOD and the AERONET observations of AOD are in good agreement, with high AOD values throughout the time period. As mentioned earlier, cloud contamination resulted in limited AOD

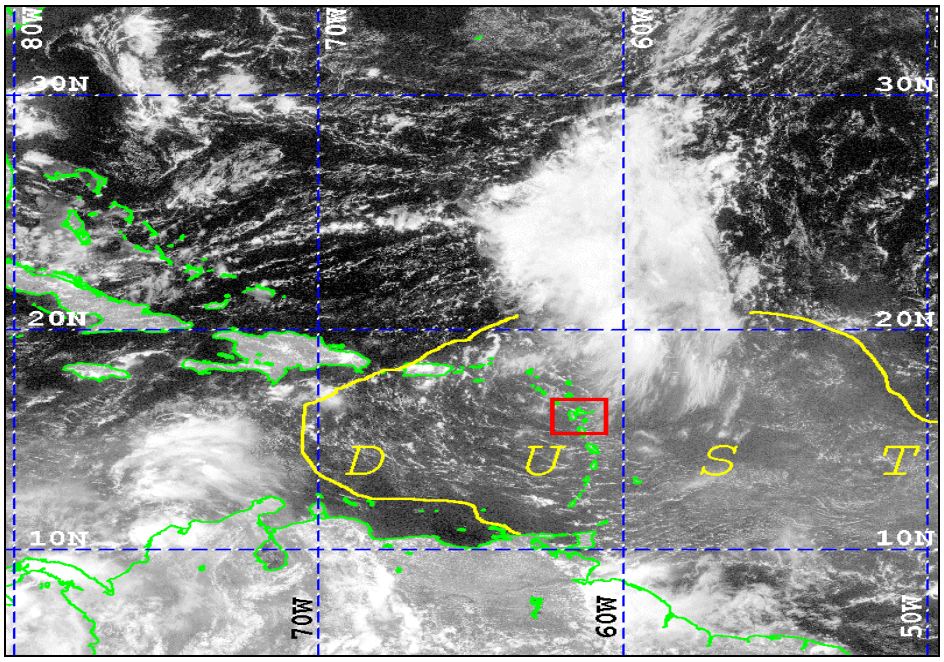

Figure 5. GOES-8 visible image on 18 September 2000 at 17:15 UTC. The annotated box surrounds the region of Guadaloupe Island. The area of aerosol dust is also annotated.

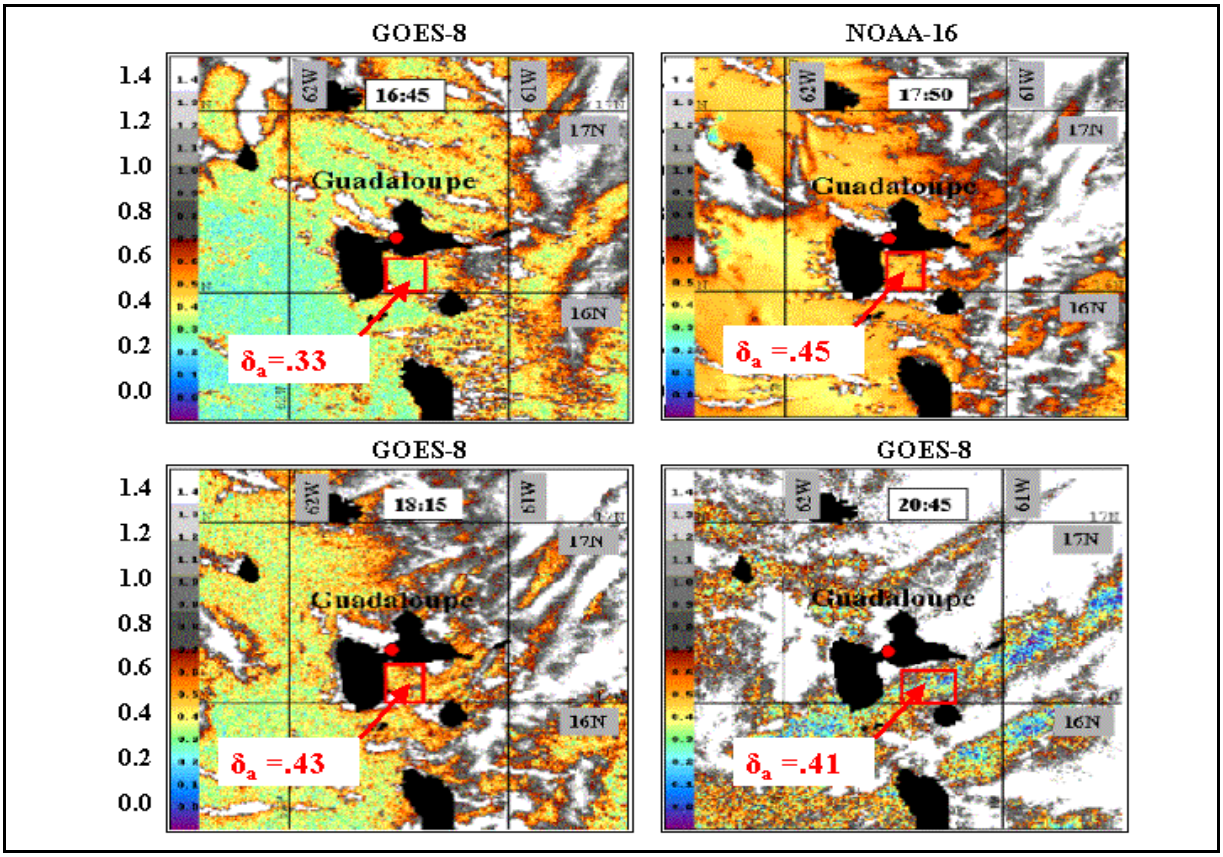

Figure 6. AOD images generated for 18 September 2001 at 17:50 UTC and 21:16 UTC from GOES-8 and NOAA-16 data, respectively. Images surround Guadaloupe Island. Pixel sizes are 1.1 km by 1.1 km and the domain is approximately 110 km by 110 km. Red boxes depict the locations where the representative AOD for that area were measured. AOD color contours are defined on the left side of each image.

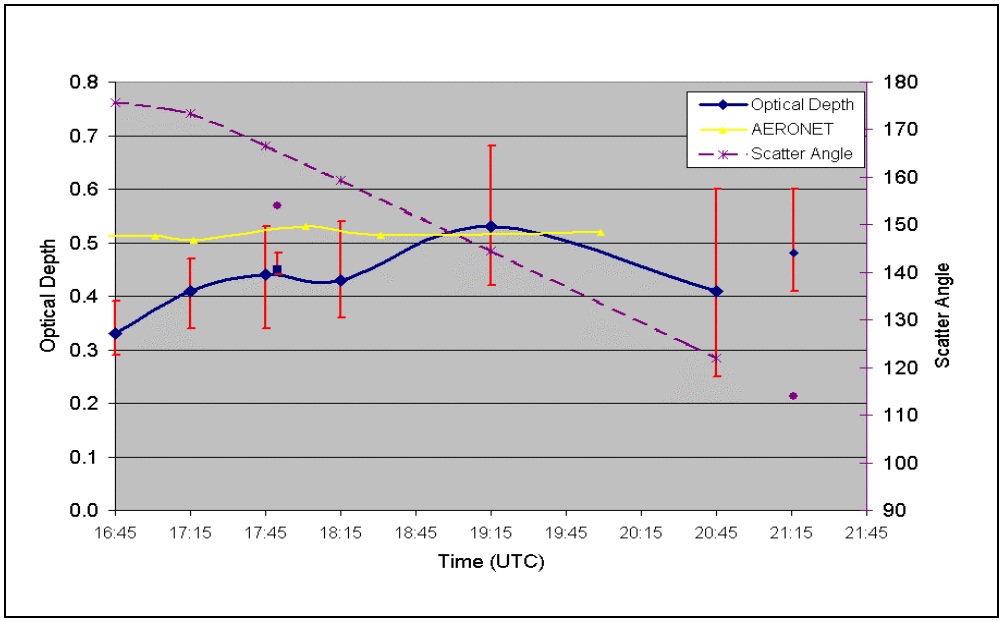

Figure 7. Chart of AOD for both satellite-derived data (navy blue dots) and AERONET observations (yellow) for 18 September 2001 over Guadaloupe Island. NOAA data are presented as individual blue dots whereas GOES-8 data are connected with a blue line. Red bars represent variability in AOD measurements. The corresponding scatter angle profile is represented as a purple dashed line.

measurements after 19:15 UTC. The lengths of the variability bars associated with GOES-8 data increased with time. As a result, the proper selection of AOD measurements became increasingly more difficult. The AOD generated from the NOAA-16 data at 17:50 UTC (AOD ~ 0.45) and the NOAA-14 data at 21:17 UTC (AOD ~ 0.48) are also in agreement with AERONET observations. Based on the scatter angle profile, local noon occurred toward the beginning of the time period (~16:45 UTC). The AOD from AERONET observations tend toward higher values than the satellite-derived AOD during the early afternoon hours. The reverse occurs later in the day.

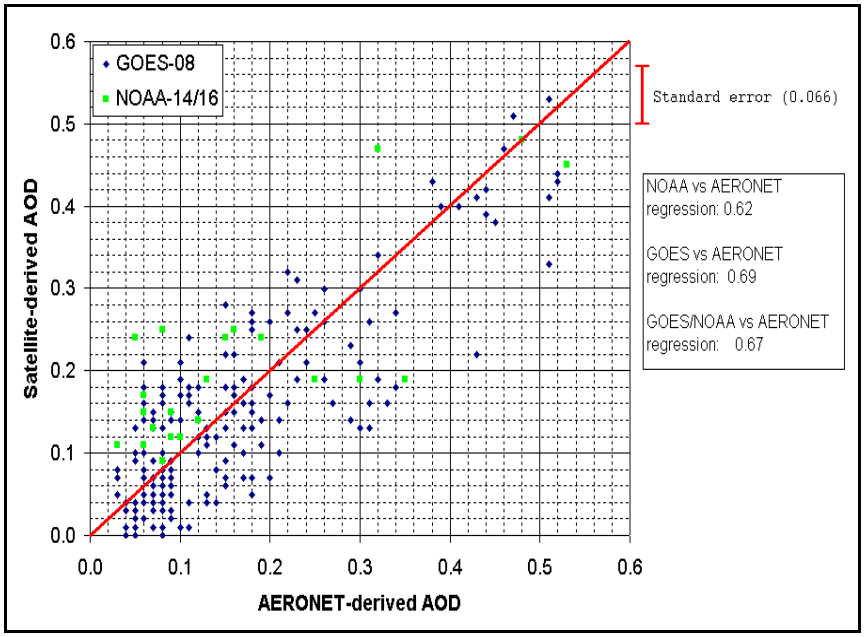

Figure 8. Comparisons between NPS-calculated AOD and AERONET-observations of AOD for 22 cases. The red line depicts one to one relationship.

4.2 *RESULTS FROM 22 CASES*

For each of the 22 cases, measurements were taken in such a way as to compare AOD between AERONET and satellite images as close to each other as possible without land or cloud contamination. For an in-depth overview of each case, please refer to the article titled: "kuciauskas_thesis.pdf" that is available at the anonymous web site: ftp://ftp.nrlmry.navy.mil/pub/receive/kuciausk.

Figure 8 compares satellite-derived AOD data with AERONET 'ground truth' observations for all 22 cases. Within low AOD conditions (δ_a < 0.2), there is a slight bias for NOAA-derived AOD values toward higher values. The GOES-derived values have a slight bias toward lower AOD values. Within dust conditions (δ_a > 0.25), there is a bias within the NPS algorithm to an underestimate AOD. Similar findings found by Smith (1998) attributed the probable cause to the "no absorption" assumption (ω_o = 1) within the NPS algorithm. As shown in Figure 33, the overall standard error for AOD measurement is 0.066. For the regression analysis, the GOES and NOAA combined results in an R^2 of 0.67. Individually, the NOAA regression is 0.62 while the GOES regression is higher at 0.67.

Another method to evaluate the performance of the NPS algorithm was to determine whether there was bias in AOD calculations due to varying geometries between the sun and satellite positions. Figure 9 is a display that categorizes several regression parameters into scatter angle categories. Due to the position of the study areas and the fixed location of the GOES-8 satellite, local noon occurs around the peaks of scatter angles (total backscatter). Therefore, in Figure 9, the scatter angle category of 170° – 180° (complete backscatter) is within the region of local noon. R2 describes the degree of correlation between satellite-derived AOD and AERONET data. For example, R2 = 0.40, indicates that 40% of the original variability of the satellite-derived AOD can be explained, with a remaining 60% of residual variability. As shown within the bar patterns of Figure 13, R^2 values are highest about 140° – 150° (R^2 ~ 0.72) and at 170° - 180° (R^2 ~ 0.76). Corresponding standard error (S.E.) values are at their lowest within the scatter angle categories of 130° - 140° and 170° - 180°, respectively. A possible explanation for the higher accuracy about 140 degrees could be that the model phase function table of values used within the NPS algorithm converge toward one value at ~140 degrees. Therefore, there are no aerosol size distribution errors at this scatter angle.

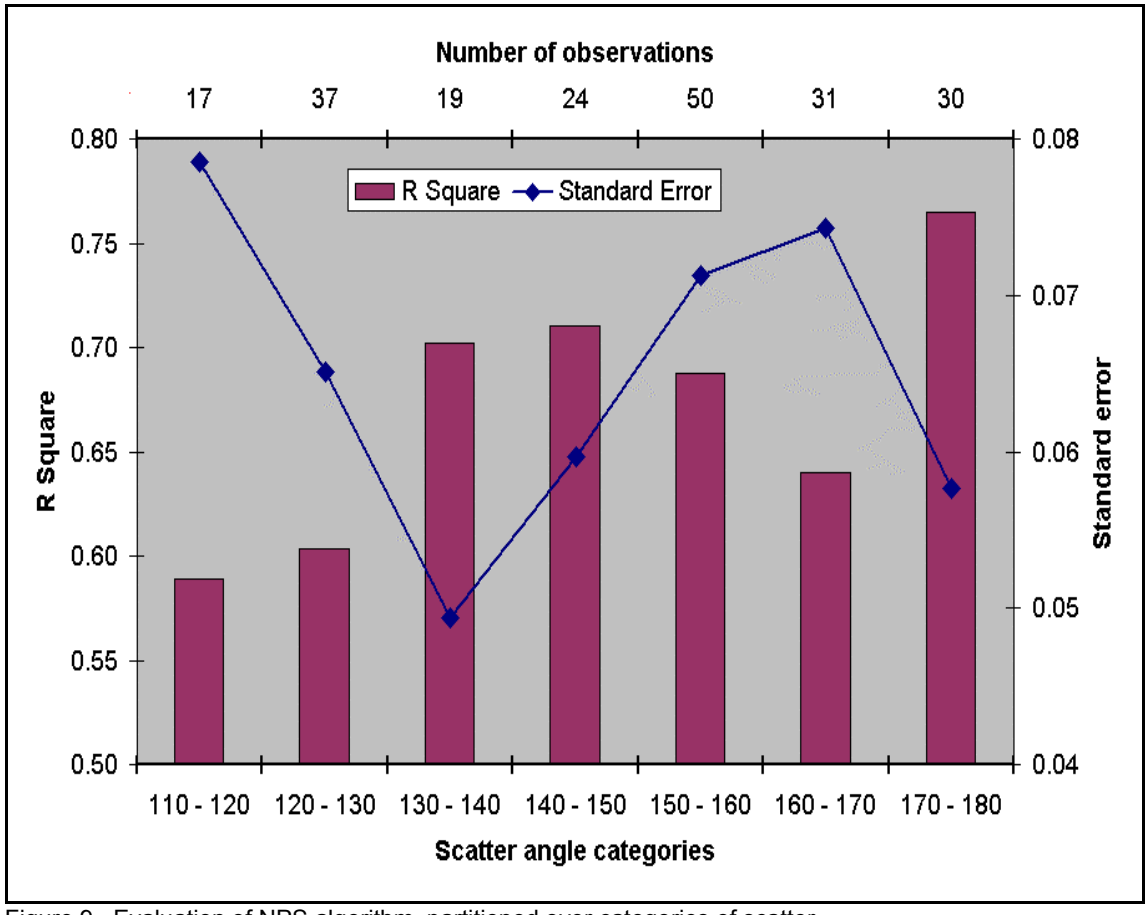

Figure 9. Evaluation of NPS algorithm, partitioned over categories of scatter.

Figure 10 displays the phase function analysis for the 22 cases within dust conditions ($\delta_a \geq 0.25$). Satellite-derived phase functions (blue dots) and the phase functions required to match the AERONET AOD (red dots) are shown. Between 140° and 180°, phase function values generated by the NPS algorithm indicate a pattern of higher curvature than that of AERONET-based phase functions. This result is consistent with work conducted by Collins *et al*. (2000) in the ACE-2 experiment off the West African coast (upstream from the PRIDE region). Beyond the scatter angle of 140°, non-spherical dust particles were observed to produce a flatter phase function shape than non-dust conditions. The NPS algorithm is based on non-dust, spherical aerosol particles. Therefore, it would be plausible to apply to the NPS algorithm a modified phase function that is flatter in the backscatter region during dust events.

5. CONCLUSIONS

A radiative transfer algorithm (NPS algorithm) that processes AOD within a cloud-free maritime atmosphere was presented for the NOAA POES AVHRR and GOES imager. This algorithm applies linearized, single-scatter theory with an estimate of bi-directional surface reflectance. Using a technique developed by Durkee *et al.* (1991), scattering phase functions are parameterized to seven aerosol size distributions by applying the ratios of channel 1 and 2 radiances (S_{12}) of the AVHRR. The S_{12} value is then translated to an aerosol model index (AMI) value that is accessed by GOES processing. Both the NOAA and GOES processing then apply the AMI to a look up table to determine the scattering phase function. The development and validation of the NPS algorithm is a continuation of the initial work performed by Brown (1997).

Unlike the AVHRR data, the GOES-8 visible radiance data required an unconventional calibration scheme. During the analysis period of this paper (July and August, 2001) signal gain factors ranging from 1.727 during the first case study (July 27, 2001) through 1.740 during the last study (September 25, 2001) were applied to the GOES raw channel 1 albedo data. In addition, preliminary comparisons of AOD between GOES and NOAA, and AERONET revealed that an additional GOES-8 channel 1 offset correction factor of $-5.5\ Wm^{-2}\ sr^{-1}\mu m^{-1}$ was necessary.

To validate the NPS algorithm, retrieved AOD data was collected from 22 cases during July and September of 2001 and compared to AERONET radiometers positioned within 3 island locations of the western Atlantic Ocean. For each case, a time series format was used to study temporal variations in AOD. Overall, the comparison dataset has a correlation coefficient of 0.67 with a standard error of 0.07. Within higher AOD cases ($\delta_a > 2.5$), the general trend was for the NPS-generated AOD values to under-estimate AERONET-observed conditions, probably due to assumptions of non-absorption applied to aerosol particles. When related to scatter angles, the NPS-generated AOD calculations performed best within the backscatter angle ranges of 130° - 140° and 170° -180°.

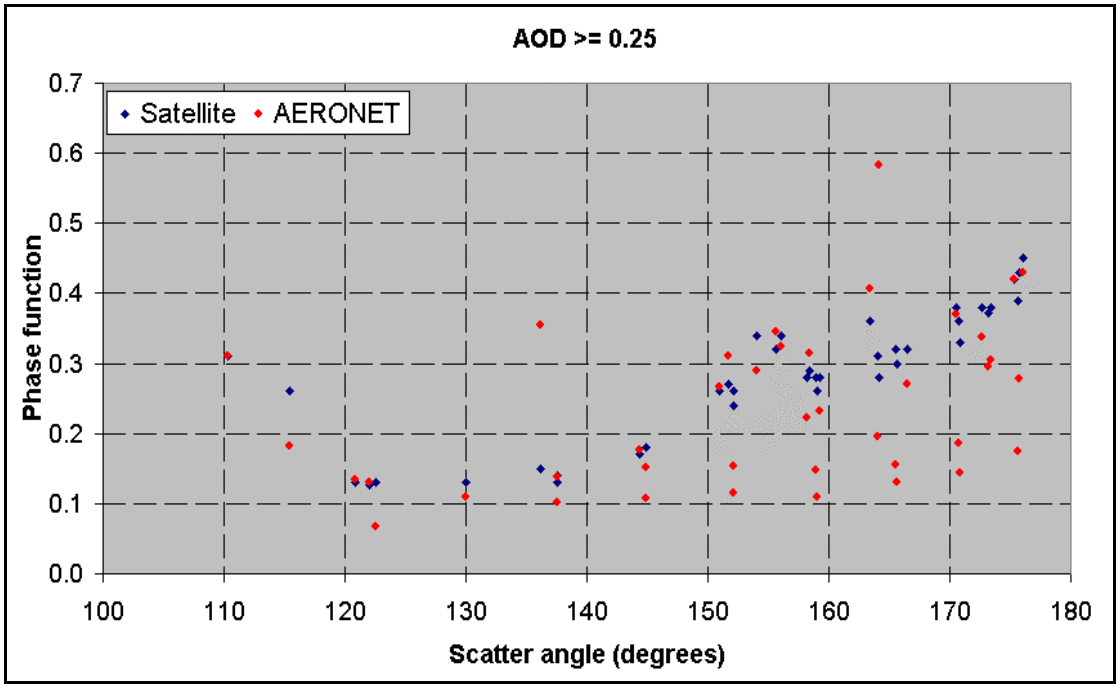

Figure 10. Comparisons of phase functions between satellite data and AERONET data for 22 cases. Figure only depicts dust conditions (AERONET AOD ≥ 0.25).

A major part of the uncertainty to the AOD processing is the proper selection of the scattering phase function. The problem with the AOD results generated from GOES data is that the aerosol conditions over a particular region were assumed to be unchanging throughout the entire time period, which might last for 8 hours. Unfortunately, trying to validate a representative aerosol distribution was beyond the scope of this study. The AOD results were apparently not very sensitive to any aerosol model assigned to the calculation.

The pattern of the NPS algorithm-generated phase functions was evaluated during the dust events ($\delta a \geq 0.25$). Between the scatter angles of 140^{o} through 180^{o}, the phase function pattern required to match AERONET observations indicated a flatter profile than that produced by the NPS algorithm on GOES and NOAA data. Collins et al (2000) confirm the AERONET-generated phase function profile for non-spherical dust aerosols compared to spherical particles assumed in the NPS algorithm.

5.1 *Ongoing AOD products generated by the NPS algorithm*

Daily products of GOES and POES-generated AOD are available for the U.S. west coast and the Caribbean Sea region, and can be viewed at: http://www.nrlmry.navy.mil/aerosol.

6. LIST OF REFERENCES

Brown, B. B., 1997: Remote measurement of aerosol optical properties using the NOAA POES AVHRR and GOES Imager during TARFOX. M.S. Thesis, Naval Postgraduate School, Monterey, CA, 73 pp.

Collins, D. R., H. H. Jonsson, J. H. Seinfeld, R. C. Flagan, S. Gassó, D. A. Hegg, P. B. Russell, B. Schmid, J. M. Livingston, E. Öström, K. J. Noone, L. M. Russell and J. P. Putaud, 2000: In situ aerosol – size distributions and clear-column radiative closure during ACE-2. Tellus, 52B, 498-525.

Durkee, P. A., F. Pfeil, E. Frost, and R. Shema, 1991: Global analysis of aerosol particle characteristics. Atmos. Env., 25A, 2457-2471.

Durkee, P. A., K. E. Nielsen, P. J. Smith, P. B. Russell, B. Schmid, J. M. Livingston, B. N. Holben, C. Tomasi, V. Vitale, D. Collins, R. C. Flagan, J. H. Seinfeld, K. J. Noone, E. Öström, S. Gasso, D. Hegg, L. M. Russell, T. S. Bates and P. K. Quinn, 1999: Regional aerosol optical depth characteristics from satellite observations: ACE-1, TARFOX and ACE-2 results. Tellus, 51B, 1-14.

Higurashi, A. T., T. Nakajima, B. N. Holben, A. Smirnov, R. Frouin, and B. Chateret, 1999: A study of global aerosol optical climatology with two channel AVHRR remote sensing. J. Climate, 13, 2011-2027.

Holben, B. N., T. F. Eck, I. Slutsker, D. Tanré, J. P. Buis, A. Setzer, E. Vermote, J. A. Reagan, Y. J. Kaufman, T. Nakajima, F. Lavenu, I. Jankowiak, and A. Smirnov, 1998: AERONET – A federated instrument network and data archive for aerosol characterization. Remote Sens. Environ., 66, 1-16.

Kuciauskas, A. P., 2002: Aerosol optical depth analysis with NOAA GOES and POES in the western Atlantic. M.S. Thesis, Naval Postgraduate School, Monterey, CA, 99 pp.

Rao, C. R. N. and N. Zhang, 1999: Calibration of the visible channel of the GOES images using the Advanced Very High Resolution Radiometer. Pre-print volume, 10th Atmospheric Radiation Conference (Madison, Wisconsin), 560-563.

Rao, C. R. N., C. J. Sullivan, and N. Zhang, 1999: Post-launch calibration of meterorlogical satellite sensors. Adv Space Res., 23, 1357-1365.